Journal of Mechanics Engineering and Automation 3 (2013) 311-324

Turbulent Energy Budgets of a Ground Vortex Flow

Jorge M.M. Barata[1], Pedro J.C.T. Santos[1], André R.R. Silva[1] and Diamantino F.G. Durão[2]

1. Dept. of Aerospace Science, University of Beira Interior, Covilhã 6200-001, Portugal

2. Lusíada Institute for Research and Development, Universidade Lusíada, Lisbon 1349-001, Portugal

Received: November 9, 2012 / Accepted: December 7, 2012 / Published: May 25, 2013.

Abstract: Turbulent kinetic energy budgets are presented for a highly curved flow generated by the collision of plane wall turbulent jet with a low-velocity boundary layer. The different terms are obtained in the vertical plane of symmetry by quadratic interpolation of the LDV (Laser Doppler Velocimetry) measurements, for a wall jet-to-boundary layer velocity ratio of 2. The results, which have relevance to flows encountered in powered-lift aircraft operating in ground effect, quantify the structure of the complex ground vortex flow. The analysis of turbulent energy equation terms using the measured data revealed that production by normal and shear stresses are both very important to the turbulent structure of the impact zone of the ground vortex. This is an indication that the modeling of turbulence of a ground vortex requires a good representation of the production by normal stresses which is most important in the collision zone.

Key words: V/STOL (vertical/short take-off and landing), ground vortex, turbulence, complex flows.

Nomenclature

h	Height of the wall jet nozzle slit
H	Distance from the nozzle exit to the ground plane
U	Mean horizontal velocity component
u'	Turbulent horizontal velocity component
U_0	Boundary layer / crossflow velocity
U_j	Wall jet velocity
u'_{rms}	*rms* of the horizontal fluctuating velocity component, $\sqrt{\overline{u'^2}}$
$\overline{u'v'}$	Reynolds shear stress
V	Mean vertical velocity component
v'	Turbulent vertical velocity component
V_j	Velocity of the jet at the nozzle exit
V_R	Boundary layer to wall jet (or crossflow to jet) velocity ratio, $V_R = U_j / U_0$
v'_{rms}	*rms* of the vertical fluctuating velocity component, $\sqrt{\overline{v'^2}}$
X	Horizontal Cartesian coordinate (parallel to the wall, pointing in the sense of the wall jet)
Y	Vertical Cartesian coordinate (normal to the wall pointing upwards

Pedro J.C.T. Santos, M.Eng., research field: aerodynamics.

André R.R. Silva, assistant professor, Ph.D., research fields: two phase flows, aerodynamics.

Diamantino F.G. Durão, full professor, Hab., Ph.D., research fields: LDA, fluid mechanics.

Corresponding author: Jorge M.M. Barata, full professor, Hab., Ph.D., research fields: aerodynamics, computational fluid dynamics, VSTOL. E-mail: jbarata@ubi.pt.

1. Introduction

Highly curved flows are quite common in nature and are frequently originated by impermeable surfaces that deflect a flow [1]. This type of complex flows is characterized by complicating influences like extra rates of strain and enhanced turbulence production through the interaction of normal stresses with normal strains. Typical practical applications can be found in impingement cooling applications in industry, as well as of the flow beneath a short/vertical take-off aircraft which is lifting off or landing with zero or small forward momentum. In this latter application, each lift jet impinge on the ground resulting in the formation of a wall jet that flows radially from the impinging point along the ground surface, interacting strongly with the ground plane. As a result, lift losses, enhanced entrainment close to the ground (suckdown), engine thrust losses following re-ingestion of the exhaust gases and in possible aerodynamic instabilities caused by fountain impingement on the aircraft underside may occur. The interaction of this wall jet with the free stream results in the formation of a highly curved flow (ground vortex, see Fig. 1) far upstream of the

Fig. 1 Representation of the ground vortex flow phenomena on the underside of V/STOL aircrafts (Joint Strike Fighter F-35 Variant B).

impinging jet that has profound influences on the flow development [2-8]. Measurements of this type of flow are very scarce, and have only been reported in the context of a secondary flow within the impinging jet flow problem. Reference 8 found that the shape, size and location of the ground vortex were dependent on the ratio between the jet exit and the crossflow velocities, and two different regimes were identified. One is characterized by the contact between the ground vortex and the impinging jet, while another is detached upstream of the impinging zone. They also report that the crossflow acceleration over the ground vortex was directly connected with the jet exit velocity, and the influence of the upstream wall jet was not confined to the ground vortex but spread upwards by a mechanism not very well known yet.

Most of the studies published so far with relevance for the V/STOL problem used small impinging distances ($h/D < 8$) and high jet-to-crossflow velocity ratios ($V_R = U_j/U_0 > 10$). Some information relevant to the flow beneath a V/STOL aircraft in ground vicinity has been provided for some limiting cases such as $h/D = 0.4$, and without the presence of a crossflow [9-10]. Others include the effect of the crossflow with a solid surface at the jet exit plane to simulate the underside of the aircraft fuselage and wings [11-13].

Among the studies published so far without the presence of the surface at the jet exit, there is some agreement that the flow includes large scale, probably coherent, unsteadiness, although there is not a consensus as to their causes. Ref. [6] reports frequency spectra obtained with hot-wire measurements that revealed broadband humps indicating very low frequency unsteadiness ($f = 4$ Hz for $h/D = 3$ and $V_R = 10$) that were attributed to the large-scale "puffing" oscillation (low-frequency pulsating behavior) of the ground vortex, and results in a significant variation in size of the ground vortex. It was found that there was no correlation between this phenomenon and any disturbances either in the crossflow, jet wake of the jet tube, the crossflow or any oscillations in the flowfield. The low frequency oscillations were, therefore, attributed to the gross features of the ground vortex flowfield itself that included some irregularities as its growth and break-up. The reported unsteadiness was found to lead to larger fluctuations in the height of the vortex which reaches more than 8 jet diameters for $V_R = 20$, with an inverse variation of the frequency which tends almost linearly to zero when V_R increases. Ref. [14] has also observed a distinct frequency oscillation for the case of a fountain flow resulting from two compressible impinging jets without an upper plate or crossflow and NPR (Nozzle Pressure Ratios), from 1.05 up to 4, and impinging heights, h/D, of 4.4.

The studies for the highest velocity ratios with a wall at the jet exit can be found in Refs. [2-5, 11-13], for single, twin, and three jets configurations. These studies report numerical and experimental results obtained with LDV for velocity ratios, $V_R = 30$, 42, and 73, and impingement heights, of $h/D = 3$, 4, and 5, for the case of a confined crossflow. The measurements of their work were concentrated in the vertical plane of the symmetry of the flow. These authors concluded that the shear layer surrounding the jets was a region of intense velocity fluctuations with maximum values located in the region of highest mean velocity gradients. In the impingement and stagnation zones associated with the formation of the ground vortex, were noted large effects of flow distortion in the turbulence structure. The analysis of each term in the conservation equation of turbulent kinetic energy revealed the

interaction between normal stresses and normal strains. Turbulent diffusion and dissipation were important in the turbulent kinetic energy budgets, particularly in these zones. It was found that along the impinging jet the production by shear stress was the largest term in the outer edge of the jet and likely to be balanced by turbulent dissipation. The distributions along the impinging jet resemble those of a turbulent free jet [15]. Along the center of the jet, the most important term was the advection or convection term, which was related to the spread of the jet, presenting a loss of turbulent energy. With the approach to the impingement zone, the authors concluded that the turbulence production was large and higher than the largest rate of production by shear stress along the impinging jet, but it occurred due to the interaction of normal stresses with normal strains and was comparable with the advection term, which represented a gain of turbulent energy. As far as diffusion and dissipation terms are concerned the authors obtained a large value, balanced by the last referred terms. This result can explain the large distortion of the mean flow in the impingement zone and the predominance of extra source term in the balance of turbulent energy due to streamline curvature. The authors verified that the budgets of turbulent kinetic energy across the radial wall jet resemble the same for a conventional wall jet [15], with the production by shear stress as the largest term and balanced by the turbulent diffusion and dissipation. The deceleration of the radial wall jet was found to be associated with an increase of the advection term, representing a gain of turbulent kinetic energy, and as in other recirculating flows the approach of the stagnation point associated with the ground vortex is characterized by a fast increase in the production of turbulent kinetic energy through the interaction of normal stresses with normal strains. Refs. [2-4, 11-13] report numerical and experimental studies for a jet-to-cross flow velocity ratio of 30 and using a plate at the exit of the jets for one, two e three impinging jets. These authors observed that the fountain upwash flow resulting from the collision of the radial wall jets was deflected by the confined crossflow. The numerical calculations of the single and twin jet flows, with QUICK scheme and k-ε turbulence model, represented the gross features of the flows. However, the method failed to predict the turbulent structure of the impingement zones and fountain flow, which is not represented by the turbulent viscosity hypothesis. The present paper presents a detailed analysis of the turbulent structure of a ground vortex flow resulting from the collision of a wall jet with a boundary layer (Fig. 1), and follows the work of Refs. [16-19], that have detected a small recirculating zone located upstream the separation point not yet reported before for this type of flows. The present flow configuration reproduces the ground vortex upstream of the stagnation point of an impinging jet through a crossflow for a high jet-to-crossflow velocity ratio relevant to V/STOL applications. The point of maximum penetration in the crossflow direction occurs in the vertical plane of symmetry where the mean transverse velocity component is zero. So, the hypothesis under study in the present work is that the formation of the second (small) vortex is due to a particular turbulent structure not yet analyzed or reported before. To avoid the influence of the impinging region a plane wall jet is produced independently using a configuration already used to study two-dimensional upwash flows [20].

The present paper presents a detailed analysis of the turbulent structure of a ground vortex flow resulting from the collision of a wall jet with a boundary layer (Fig. 1), and follows the work of Refs. [16-19], that have detected a small recirculating zone located upstream the separation point not yet reported before for this type of flows. The present flow configuration reproduces the ground vortex upstream of the stagnation point of an impinging jet through a crossflow for a high jet-to-crossflow velocity ratio relevant to VSTOL applications. The point of maximum penetration in the crossflow direction occurs

in the vertical plane of symmetry where the mean transverse velocity component is zero. So, the hypothesis under study in the present work is that the formation of the second (small) vortex is due to a particular turbulent structure not yet analyzed or reported before. To avoid the influence of the impinging region a plane wall jet is produced independently using a configuration already used to study two-dimensional upwash flows [20].

The wall jet collides with the boundary layer produced using a conventional wind tunnel giving rise to a ground vortex, which can be studied for different velocity ratios between the wall jet and crossflow. Using the theory of turbulent jets and the distance to the separation point, it is possible to establish a relationship between the wall jet velocity and the velocity at the jet exit. In this work, and according to our hypothesis, a velocity ratio between the wall jet and the crossflow (V_R) of 2.0 was used, because it corresponds to a regime with the presence of the small vortex. The mean and turbulent velocities and the Reynolds shear stress data was used to calculate the turbulent kinetic balances to understand the complex flow in the collision zone. This paper is organized in four sections, including the present introduction. Section 2 describes the experimental method and procedures, and section 3 presents the results. The final section summarizes the main findings and conclusions of this work.

2. Experimental Method and Procedures

The flow configuration studied is schematically shown in Fig. 2. The figure is divided into two regions. One region is near the impinging jet while the other region is the area where the wall jet collides with the crossflow. The second region will be analyzed in the present paper. Three-dimensional effects created by skewing of pre-existing spanwise vorticity are eliminated, and makes our data particularly interesting to assess the turbulent or transient effects near the separation point of the ground vortex where the transverse velocity component is null.

The recommendations of Ref. [21] for open circuit wind tunnels were followed throughout all the design process especially for the boundary layer part of the flow. A fan of 15 KW nominal power drives a maximum flow of 3000 m^3/h through the boundary layer and the wall jet tunnels of 300 × 400 mm and 40 × 400 mm exit sections, respectively. The facility was built to allow variable heights of the wall jet exit from 15 up to 40 mm, but in the present study a constant value of 16 mm was used.

The origin of the horizontal, X, and vertical, Y, coordinates is taken near the visual maximum penetration point. The X coordinate is positive in the wall jet flow direction and Y is positive upwards.

The present results were obtained at the vertical plane of symmetry for a wall jet mean velocities of U_j = 13.7 m/s and mean boundary layer velocity of U_o = 6.9 m/s corresponding to a velocity ratio, V_R, of 2.0.

The velocity field was measured with a two-color (two-component) laser-Doppler velocimeter (Dantec Flowlite 2D), which comprised a 10 mW He-Ne and a 25 mW diode-pumped frequency doubled Nd:YAG

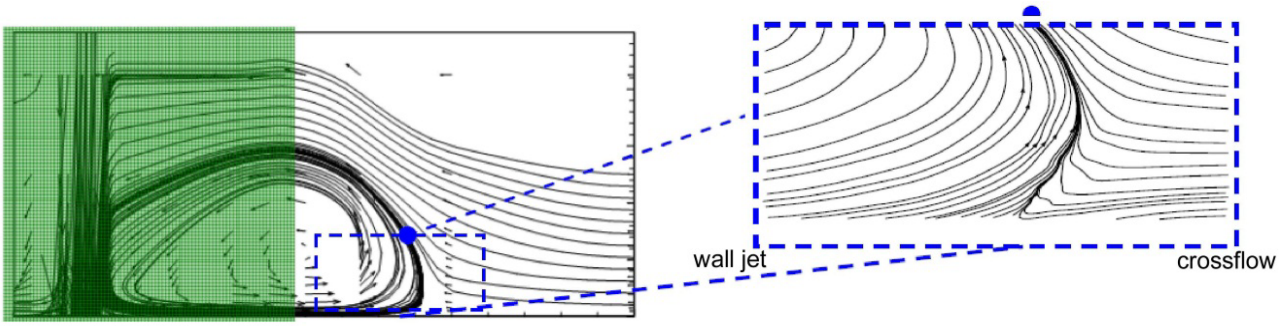

Fig. 2 Diagram of the flow studied (dashed area).

Table 1 Characteristics of the Laser-Doppler velocimeter.

Wave length, λ (nm)	633 (He-Ne)	532 (Diode Laser)
Focal length of focusing lens, f (mm)	400	400
Beam diameter at e^{-2} intensity (mm)	1.35	1.35
Beam spacing, s (mm)	38.87	39.13
Calculated half-angle of beam intersection, θ (^{o})	2.78	2.8
Fringe spacing, δ_f (μm)	6.53	5.45
Velocimeter transfer constant, K (MHz/ms^{-1})	0.153	0.183

lasers, sensitivity to the flow direction provided by frequency shifting from a Bragg-cell at f_o = 40 MHz, a transmission and backward scattered light collection focal lens of 400 mm. The half-angle between the beams was 2.8^o and the calculated dimensions of the axis of the measuring ellipsoid volume at the e^{-2} intensity locations were 135 × 6.54 × 6.53 μm and 112 × 5.46 × 5.45 μm respectively. The horizontal, U, and the vertical, V, mean and turbulent velocities together with the shear stress, $\overline{u'v'}$, were determined by a two-channel Dantec BSA F60 processor. The principal characteristics of the laser-Doppler velocimeter are summarized in Table 1. The seeding of the flow was obtained with a smoke generator with particles of 0.1-5 μm. The number of the individual velocity values used in the measurements to form the averages was always above 10,000, although statistical convergence mean, turbulence quantities and shear stress was achieved when the sample contained more than 3,500 points. As a result, the largest statistical (random) errors were 1.5% and 3%, respectively for the mean and variance values for a 95% confidence interval following the analysis of Ref. [22]. The transmitting and collecting optics is mounted on a three-dimensional traversing unit, allowing the positioning of the center of the control volume within of ±0.1 mm.

3. Results

The analysis of turbulent kinetic energy resulting from the collision of wall jet with a boundary layer is presented and discussed in this section. Turbulent kinetic energy balances were obtained in vertical plane of symmetry by quadratic interpolation of the LDV measurements, the mean and turbulent velocity characteristics. The terms in the equation of transport of the kinetic energy were associated according to Eq. (1).

$$\underbrace{U\frac{\partial k}{\partial X}+V\frac{\partial k}{\partial Y}}_{\text{convection}}=\underbrace{-\overline{u'^2}\frac{\partial \overline{U}}{\partial X}-\overline{v'^2}\frac{\partial \overline{V}}{\partial Y}}_{\text{production by normal stresses}}\underbrace{-\overline{u'v'}\left(\frac{\partial \overline{U}}{\partial Y}+\frac{\partial \overline{V}}{\partial X}\right)}_{\text{production by shear stresses}}\overbrace{-\frac{\partial}{\partial X}\left(\overline{k'u'}+\frac{\overline{p'u'}}{\rho}\right)-\frac{\partial}{\partial Y}\left(\overline{k'v'}+\frac{\overline{p'v'}}{\rho}\right)}^{\text{diffusion}}\overbrace{-\varepsilon}^{\text{dissipatio n}} \quad (1)$$

The convection term was calculated by the approximation of k by $\frac{3}{4}\left(\overline{u'^2}+\overline{v'^2}\right)$ and the sign corresponds to Eq. (1) which has the signification of turbulent kinetic energy local gain when presents negative values and turbulent kinetic energy local loss when presents positive values. The production of turbulent kinetic energy by normal stresses and production by shear stresses are exact values and when they present positive values they represents kinetic energy gain. The terms of diffusion and dissipation are aggregated in the equation and horizontal and vertical profiles as other terms. They are obtained by difference of other equation terms since it was not possible to measure during the execution of the experimental work. Their sign has the same signification that in the case of the production terms, when they presents negative values there is correspondence to a kinetic energy loss.

The terms in Eq. (1) were obtained directly from the experimental measurements, and the spatial derivates were calculated using quadratic interpolation. As already mentioned before, the errors in the mean values and Reynolds stresses were less than 1.5% and 3%, respectively. The errors in the calculation of k are less

than 6%. The errors in the spatial derivates are of the order of 2% (6% × 0.25%), as a consequence of the second order approximation.

The analysis of kinetic energy budgets is made using horizontal and vertical profiles together with contours. The horizontal profiles of turbulent kinetic energy budgets are presented for the three horizontal main regions of the flow that are represented in Fig. 3 together with streaklines and mean velocity vectors. The first horizontal region, Horizontal Region 1, corresponds to the vicinity of the wall and includes the interaction zone resulting from the collision between the wall jet and the boundary layer. The second horizontal region, Horizontal Region 2, corresponds to an intermediate region that contains a larger part of the deflected flow resulting from the collision of the two opposed flows, and it is defined from Y = 25 mm to Y = 85 mm. The last region is the Horizontal Region 3 and presents the flow in the region far from the wall.

Fig. 4 presents the horizontal profiles of turbulent kinetic energy in Horizontal Region 1 near the wall. The convection term is always near zero from the wall jet side to the boundary layer side with a little negative variation in the zone corresponding to the collision between wall jet and boundary layer (X = -20 mm to X = 40 mm). This result corresponds to a small local loss of turbulent kinetic energy in this zone that tends to decrease with the distance to the wall. At Y < 24 mm the convective term tends to be zero in the collision zone defined from X = -20 mm to X = 40 mm. Between

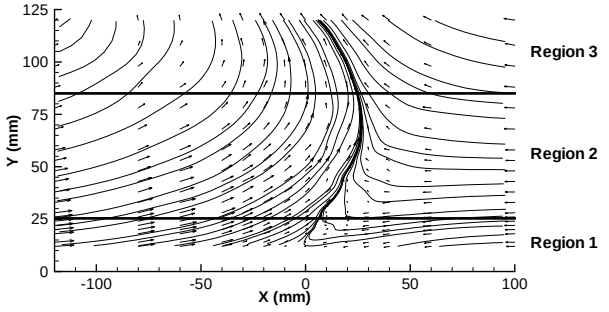

Fig. 3 Characteristic horizontal regions of the flow. Horizontal Region: 1—Vicinity of wall, *Y* = 12-25 mm; 2—Intermediate region, *Y* = 25-85 mm; 3—Region far from the wall, *Y* > 85 mm.

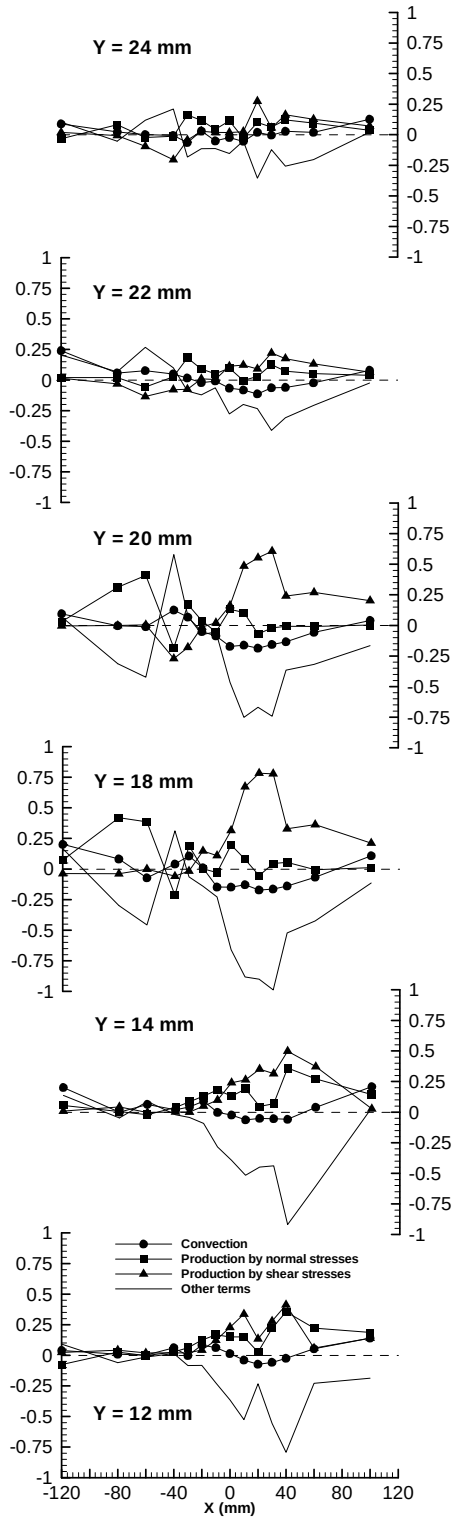

Fig. 4 Horizontal profiles of turbulent kinetic energy in Horizontal Region 1.

Y = 12 mm and Y = 20 mm it can be observed significant variations in remain equation of turbulent kinetic energy terms. In the collision zone, the

production by shear stresses is always higher than the production by normal stresses. This can be explained by the high values of shear stresses that occur in this zone between $Y = 12$ mm and $Y = 30$ mm. There is also a significant production by normal stresses in the vicinity of wall $Y = 14$ mm and $Y = 12$ mm due to the high values of horizontal normal stresses, but this contribution has tendency to decrease 20 mm $< Y <$ 22 mm. In the collision zone, the production of turbulent kinetic energy by shear stresses tends to be balanced by the loss of turbulent kinetic energy by diffusion and dissipation. However, the magnitude of the peaks tends to decrease with the distance to the wall. According to these profiles, in the region defined by -20 mm $< X <$ 40 mm the production of turbulent kinetic energy is essentially due to normal stresses. In the wall jet side the production of turbulent kinetic energy is nearly zero, but some variations occurs for $Y = 18$ mm and $Y = 22$ mm. There is a small local loss by convection, but there is a significant loss caused by the other terms of equation is balanced by the production by the shear stresses. This region corresponds to the boundary between the wall jet and the free flow, and the interaction between them can cause such variations. In the boundary of the collision zone at -60 mm $< X <$ -20 mm there are signal variations of the production by shear stresses accompanied reciprocally by the other terms. The variations of signal can be attributed to the instabilities of the flow due to its deflection and the collision between the wall jet and the boundary layer. In relation to the boundary layer side there is a small local loss of turbulent kinetic energy by convection that tends to be zero far away from the wall.

Fig. 5 shows horizontal profiles of the turbulent kinetic energy in the intermediate Horizontal Region 2. The production of kinetic energy by convection remains near zero from the wall jet side to the boundary layer side. This region is located out of the wall jet influence, so the turbulent kinetic energy is practically zero, but increasing with the distance to the wall. The same result is obtained in the boundary layer side. The kinetic energy associated with the boundary layer is more intense in the proximity of the wall and tends to zero far from the wall ($Y > 26$ mm). It is in the region of the deflected flow that results from interaction of the wall jet with the boundary layer that the kinetic turbulent energy suffers more significant oscillations. The other terms with the production by shear stresses term have significant oscillations between positive and negative peaks in this region. Near the wall at $Y = 53$ mm there is a region between $X = 5$ mm and $X = 35$ mm where the term of production by shear stress represents a loss of turbulent kinetic energy. In general the term of production by normal stresses is the dominant term, and is comparatively more important than the corresponding values observed in Horizontal Region 1.

In Horizontal Region 3 (Fig. 6), production is in general equilibrium with dissipation which indicates that turbulent kinetic energy models based on the eddy viscosity concept would give reasonable results. The convection term is very small when compared with the other terms.

The analysis of the turbulent kinetic energy vertical profiles is made for three vertical regions of the flow that are represented in Fig. 7. The first vertical region, Vertical Region 1, includes mainly the wall jet flow and the ground vortex center. The Vertical Region 2 corresponds to the most important region of flowfield since contains the interaction that results from the collision between the wall and the boundary layer together with the secondary vortex identified by Ref. [17], and also identified in the horizontal and vertical profiles of mean velocity components U and V. The same region also contains the deflected flow which forms due to the collision of the two types of flows presented. The last region, Vertical Region 3, represents the boundary side, and shows some influence on the wall jet flow.

Fig. 8 presents the vertical profiles of turbulent kinetic energy budgets in the Vertical Region 1 that includes the wall jet and the center of ground vortex.

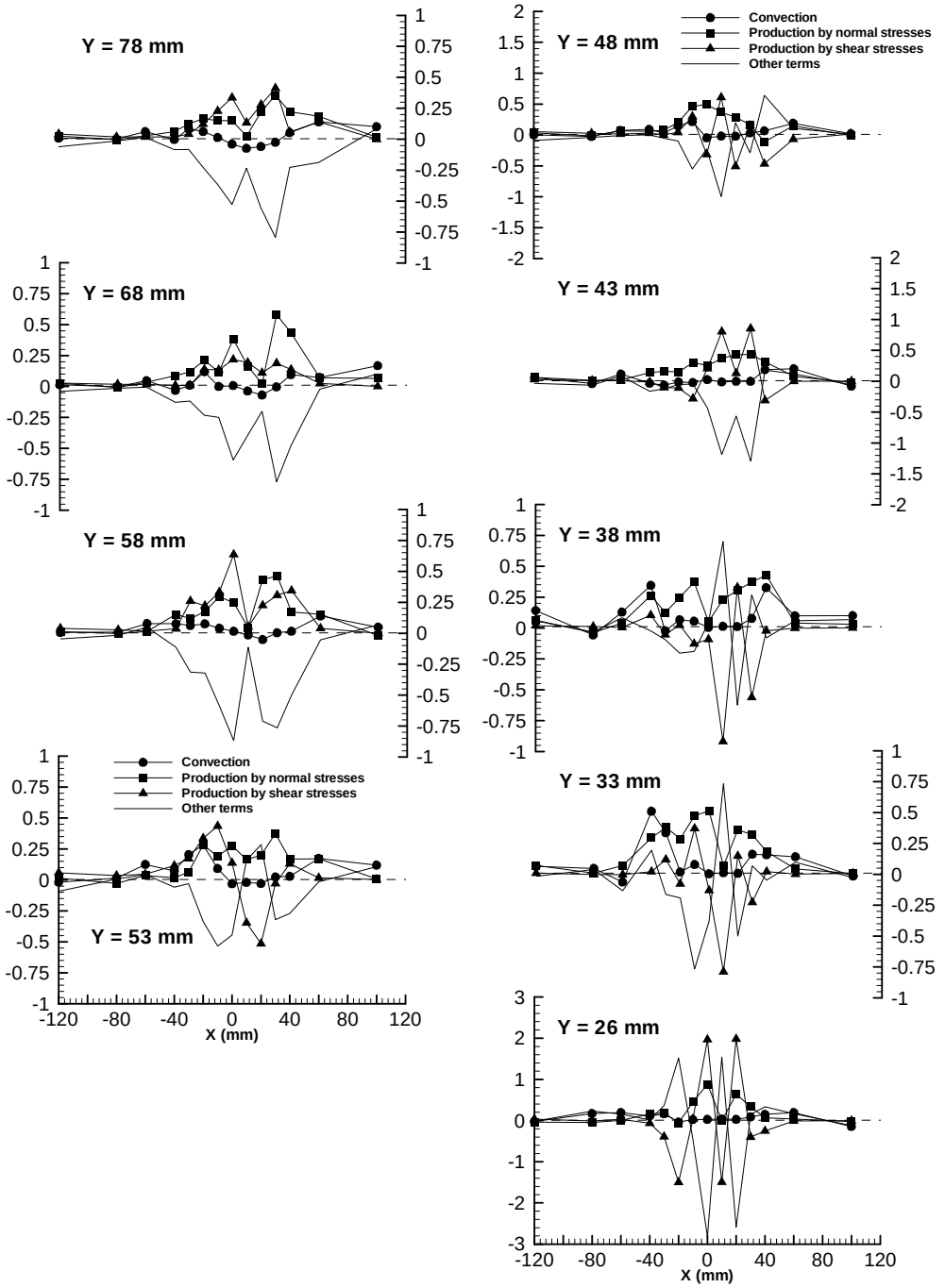

Fig. 5 Horizontal profiles of turbulent kinetic energy in Horizontal Region 2.

Far away from wall the terms of turbulent kinetic energy are nearly zero, since the flow in this zone it is not affected by the development and growth of the wall jet. However, near the deflected flow and collision zones (-40 mm < X < -20 mm) some oscillations in the terms of the turbulent kinetic energy equation are observed. Near the wall, the terms of turbulent kinetic energy suffer significant oscillations. At the wall jet exit the production by normal stresses is balanced by the production by shear stresses. The convective term and the diffusion and dissipation terms are relevant in the turbulent kinetic energy budgets, with the production by other terms not balancing the energy loss due to the convective term. Approaching the collision

zone, the convective term tends to zero and the production of turbulent kinetic energy by normal stresses becomes preponderant, and it is balanced by diffusive and dissipation terms. The increment of production by normal stresses can be explained by the importance of shear strains $\frac{\partial U}{\partial X}$ and $\frac{\partial V}{\partial Y}$ near the wall and by the significant values of normal stresses in this zone (See Ref. [17]). Near the collision zone at -40 mm <X < -20 mm significant oscillations exist in the turbulent kinetic energy terms. These oscillations may be influenced by the instabilities that occur in the collision zone and deflected flow. Near the wall, the diffusive and dissipative terms assume a great importance to the production of turbulent kinetic energy and they are balanced by the loss caused by the term of production by shear stresses. This last term becomes significant in this region, -40 mm < X < -20 mm, due to the presence of high values of shear stress, $\overline{u'v'}$, as reported by Refs. [17, 19]. The convective term represents a significant turbulent kinetic energy loss that tends to be smaller near the collision zone. This loss is balanced by the gain resulting of production by normal stresses, because in this zone at X = -40 mm, X = -30 mm and X = -20 mm the values of normal stresses are significant as showed by Ref. [19].

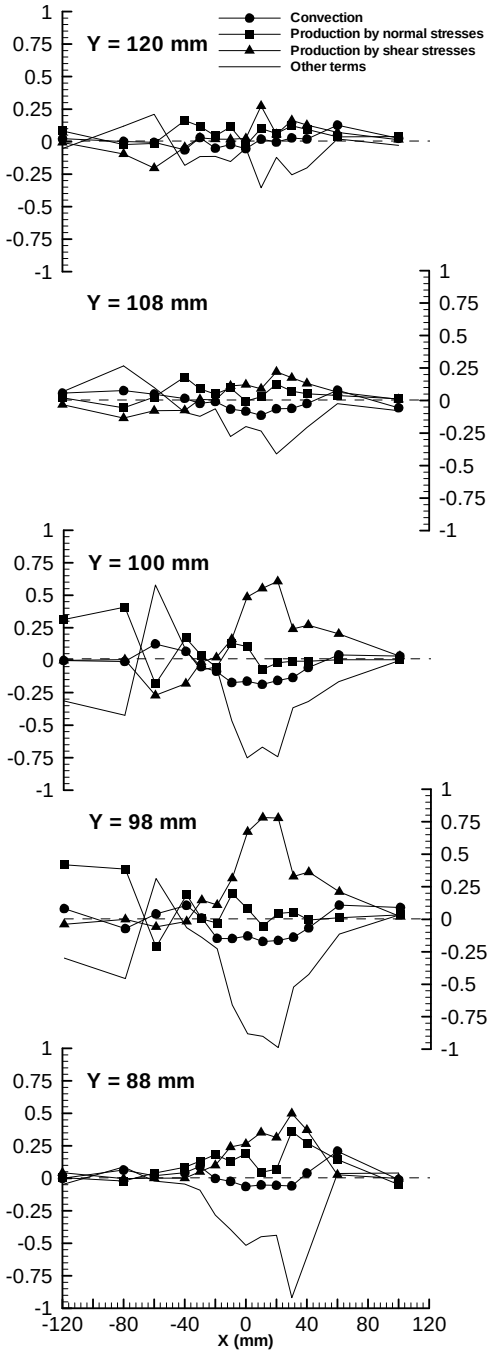

Fig. 6 Horizontal profiles of turbulent kinetic energy in Horizontal Region 3.

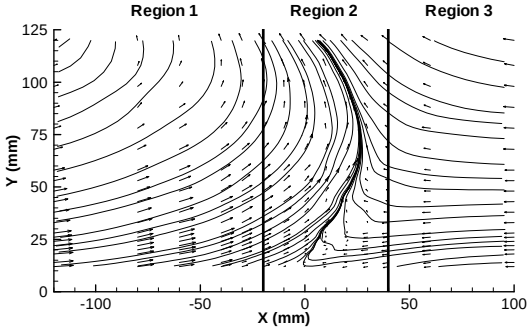

Fig. 7 Characteristic vertical regions of the flow. Vertical Region: 1—Region of the wall jet side and that contains the center of the ground vortex; 2—Region of the collision zone between the wall jet and the boundary layer and that contains the deflected flow resulting from the collision; 3—Region of the boundary layer side.

The vertical profiles of turbulent kinetic energy budgets in the interaction zone due to the collision between the wall jet and the boundary layer are presented in Fig. 9, Vertical Region 2. This zone allows the understanding of the turbulent structure created by the interaction between the two opposed flows. In Vertical Region 2 the convective term does not represents any significant contribution to the loss or gain of turbulent kinetic energy, since it remains zero

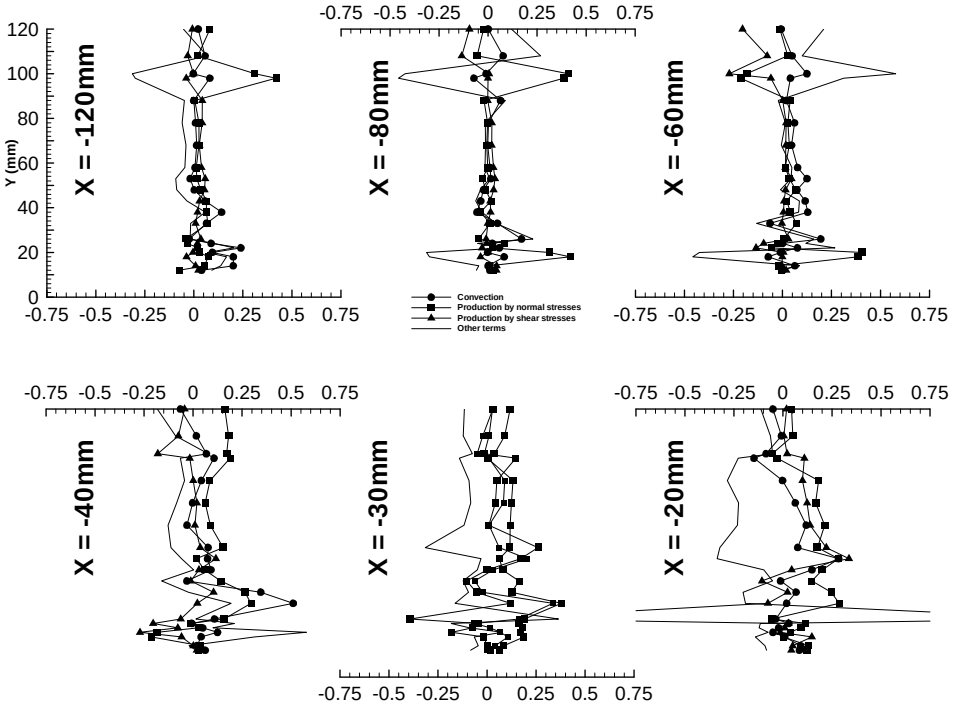

Fig. 8 Vertical profiles of turbulent kinetic energy budgets in Vertical Region 1 (wall jet side).

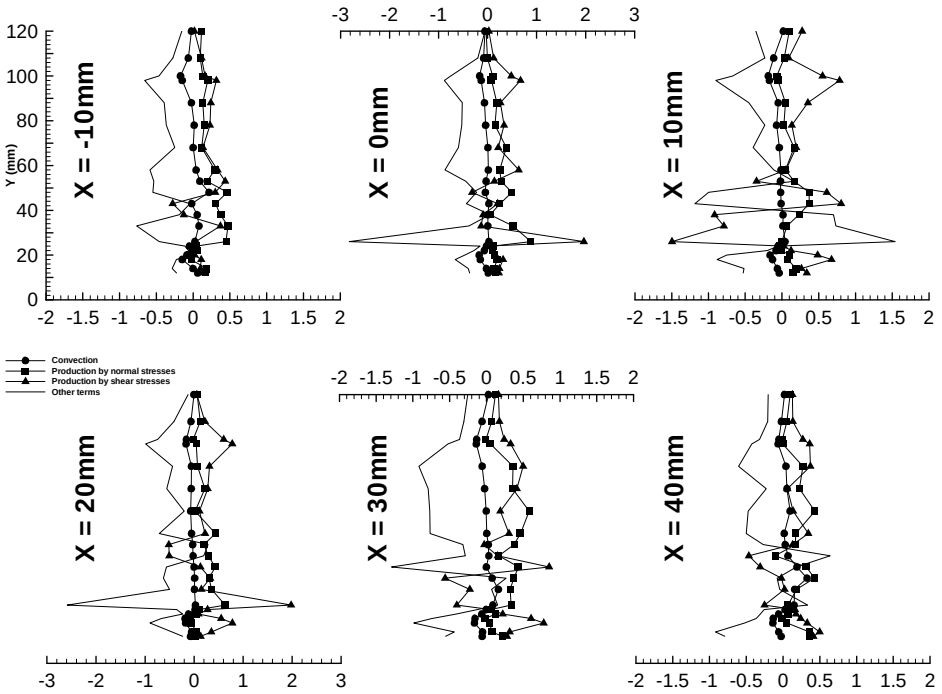

Fig. 9 Vertical profiles of turbulent kinetic energy budgets in Vertical Region 2 (collision and deflected flow zones).

from the wall vicinity ($Y < 25$ mm) to the region far away from the wall ($Y > 85$ mm). However, near the boundary layer side at $X = 30$ mm and $X = 40$ mm, and for $Y < 25$ mm a small contribution of the convective term to the production of kinetic energy exists. For this zone there is a local gain of turbulent kinetic energy by convection contrasting to the wall jet zone. According to the profiles, the diffusive and dissipative term and

the production by shear stresses become predominant, with higher values when compared with the Vertical Region 1. However, with exception of X = 10 mm vertical profile, the production of turbulent kinetic energy by shear stresses tends to be balanced by the loss of turbulent kinetic energy by diffusion and dissipation. This loss of energy is smaller in the border of the boundary layer (X = 30 mm and X = 40 mm) accompanied by a reduction in production by shear stresses. This behavior is verified along of vertical profiles between Y = 12 mm and Y = 120 mm. In this zone from X = -10 mm to X = 40 mm the shear stresses $\overline{u'v'}$ are larger when compared to the other vertical zones. This result can explain the predominance of the term production by shear stresses in this zone. Near the wall at Y < 25 mm, the production of turbulent kinetic energy is due to convection and normal stresses, since these terms present negative values and positive values, respectively. The contribution of the convective term to the production of turbulent kinetic energy is smaller than the production due to the normal stresses and shear stresses. So, the collision zone between the wall jet and the boundary layer presents a pattern similar to a wall jet. In the region far from the wall (Y > 25 mm) since the convective term is practically zero, the production of the turbulent kinetic energy is due to the normal stresses. Near the boundary layer (for 30 mm < Y < 50 mm) the convective term contributes to a small energy loss. The production of turbulent kinetic energy (essentially by normal stresses in this region far away from the wall) can be explained by the maximum and highest values of normal stresses that were reported by Refs. [17, 19] for this region. Near X = 10 mm there is a zone where the small vortex identified by Ref. [19] can be the cause for the variation of diffusive and dissipative term and production by shear stresses term in turbulent kinetic energy. These terms have an opposite behavior in relation to the other profiles in the collision zone, since there is a gain of kinetic energy due to diffusion and dissipation that is balanced by a loss by shear stresses.

Fig. 10 shows vertical profiles of turbulent kinetic energy in the Vertical Region 3 where the influence of boundary layer is dominant. In the vicinity of wall Y < 25 mm, the production of turbulent kinetic energy by convection, normal stresses and shear stresses, is not sufficient to avoid the loss of energy by diffusion and dissipation. Far away from the wall Y > 25 mm, the diffusive and dissipative term tend to balance the production by shear stresses term, and the production of turbulent kinetic energy by normal stresses balance the loss of energy by convection.

Figs. 11-14 present the contours of turbulent kinetic energy terms due to convection, production by normal stresses, production by shear stresses and the other terms, respectively. The contours together with the pathlines were computed from the vertical profiles presented in Figs. 8-10.

Fig. 11 shows a local gain of turbulent kinetic energy by convection in the collision zone of the two opposed flows, -10 mm < X < 40 mm and Y < 25 mm. In the

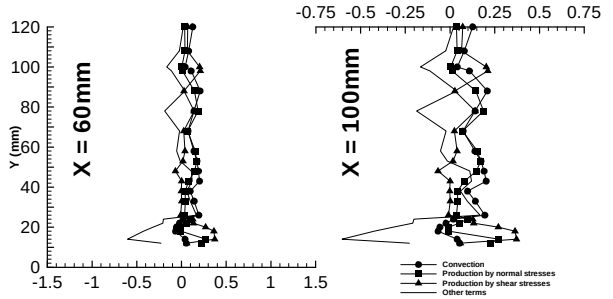

Fig. 10 Vertical profiles of turbulent kinetic energy in Vertical Region 3 (boundary layer side).

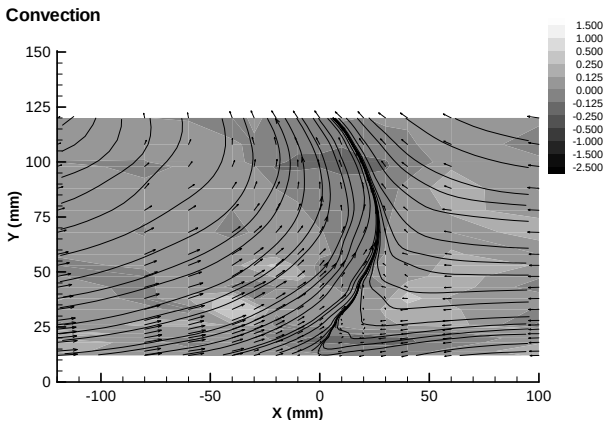

Fig. 11 Contours of the turbulent kinetic energy production, *k*, by convection.

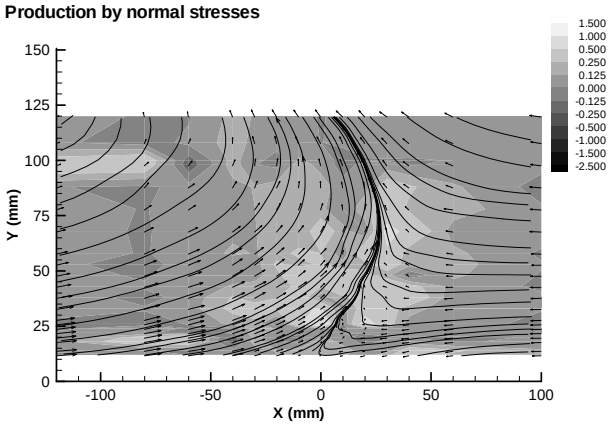

Fig. 12 Contours of the turbulent kinetic energy production, *k*, by normal stresses.

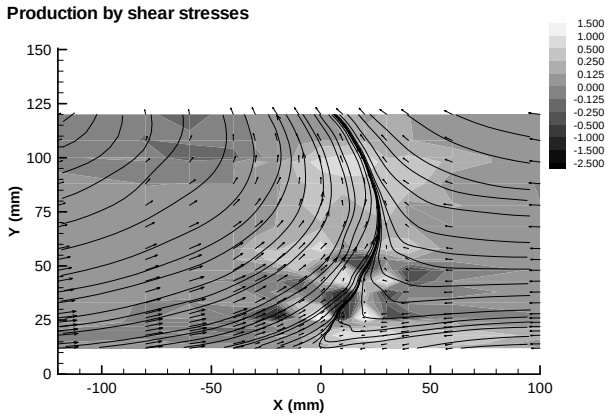

Fig. 13 Contours of the turbulent kinetic energy production, *k*, by shear stresses.

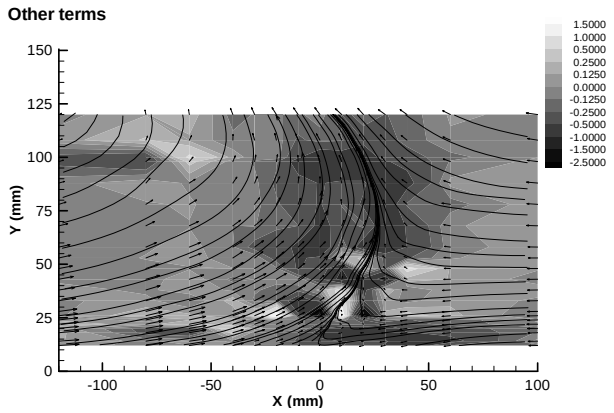

Fig. 14 Contours of the turbulent kinetic energy production, *k*, by diffusive and dissipative term (other terms).

region of the deflected flow the convective term not presents any significant contribution to the loss or gain of turbulent kinetic energy.

Figs. 12 and 14 show that near the boundary of the collision zone (from X = -80 mm to X = -40mm) the production of turbulent kinetic energy by normal stresses becomes preponderant with tendency of to be in equilibrium with the diffusive and dissipative terms. The vertical profiles of Fig. 8 show significant oscillations in the terms of turbulent kinetic energy, in the zone defined by -40 mm < X < -20 mm and 25 mm < Y < 30 mm. These oscillations can be associated with the instabilities that occur in the collision and flow deflection zones. The diffusive and dissipative terms (Fig. 14) are important to the production of turbulent kinetic energy and are balanced by the loss caused by the shear stress production term (Fig. 13).

Figs. 13-14 show that in the collision zone -10 mm < X < 40 mm, the diffusive term together with dissipative term and the production by shear stresses become predominant, and the production of turbulent kinetic energy tends to be balanced by the loss of turbulent kinetic energy by diffusion and dissipation. In the same zone and near the wall (Y < 25 mm) the production of turbulent kinetic energy is mainly due to convection (Fig. 11) together with a contribution of production by normal stress (Fig. 13). The small contribution of convective term to the production of turbulent kinetic energy is smaller than the production due to normal stresses and shear stresses in this zone. This reveals that the deflected flow presents a behavior similar to a typical wall jet.

The region near the wall at X = 10 mm position is characterized by important instabilities due to the collision of the two opposed flows and due to the existence of the small vortex identified by Ref. [17]. These phenomena can be an explanation for the variation of diffusive and dissipative term together with the production by the shear stresses term (Figs. 13-14), respectively. However, the gain of kinetic energy due to diffusion and dissipation is balanced by a loss by shear stresses.

7. Conclusions

The analysis of turbulent kinetic energy resulting

from the collision of wall jet with a boundary layer were presented and discussed with horizontal and vertical profiles together with contours for a wall jet-to-boundary layer velocity ratio of 2.

The turbulent kinetic energy balances revealed that in the collision zone of the wall jet with the boundary layer there is a local gain of energy by convection. In the region of the deflected flow the convective term not presents any significant contribution to the loss or gain of turbulent kinetic energy.

The results revealed that in the collision zone the diffusive and dissipative term and the production by shear stresses term become predominant and the production of turbulent kinetic energy tends to be balanced by the loss by diffusion and dissipation. In the same zone near to the wall, the production of turbulent kinetic energy is by convection, by normal and shear stresses. The small contribution of convective term to the production of turbulent kinetic energy is less than the production due to the normal stresses and shear stresses.

The collision zone between the wall jet and the boundary layer presents a behavior similar to a wall jet. In general the results indicate that the modeling of turbulence of a ground vortex requires a good representation of the production by normal stresses, which is important in the collision zone.

Acknowledgments

The present work has been performed in the scope of the activities of the AeroG-Aeronautics and Astronautics Group of the Portuguese Associate Laboratory in Energy, Transport and Aeronautics.

The financial support of the FCT-Fundação para a Ciência e Tecnologia of the Portuguese Ministry of Science under Contract nº PTDC/EME/-MFE/ 102190/2008 is gratefully acknowledged.

References

[1] I.P. Castro, P. Bradshaw, The turbulence structure of a highly curved mixing layer, J. Fluid Mech. 73 (2) (1976) 265-304.

[2] J.M.M. Barata, D.F.G. Durão, M.V. Heitor, Experimental and numerical study on the aerodynamics of jets in ground effect, in: 10th Symposium on Turbulence, September 22-24, 1986, Rolla, Missouri.

[3] J.M.M. Barata, D.F.G. Durão, M.V. Heitor, The turbulent characteristics of a single impinging jet through a crossflow, in: 6th Symposium on Turbulent Shear Flows, September 7-9, 1987, Toulouse.

[4] J.M.M. Barata, D.F.G. Durão, M.V. Heitor, Turbulent energy budgets in impinging zones, in: 8th Symposium on Turbulent Shear Flows, September 9-11, 1991, Munich.

[5] W.R.V. Dalsem, A.G. Panaras, J.L. Steger, Numerical investigation of a jet in a ground effect with a crossflow, in: International Powered Lift Conference, SAE Paper 872344, December 7-10, 1987, Santa Clara, California.

[6] J.M. Cimbala, M.L. Billet, D.P. Gaublomme, J.C. Oefelein, Experiments on the unsteadiness associated with a ground vortex, Journal of Aircraft 28 (4) (1991) 261-267.

[7] K. Knowles, D. Bray, The ground vortex formed by impinging jets in crossflow, in: AIAA 29th Aerospace Sciences Meeting, AIAA Paper 91-0768, January 7-10, 1991, Reno, Nevada.

[8] J.M.M. Barata, D.F.G. Durão, Laser-Doppler measurements of impinging jets through a crossflow, Experiments in Fluids 36 (5) (2004) 117-129.

[9] K.R. Saripalli, Visualization of multijet impingement flow, AIAA Journal 21 (1983) 483-484.

[10] K.R. Saripalli, Laser Doppler velocimeter measurements in 3D impinging twin-jet fountain flows, Turbulent Shear Flows 5 (1987) 147-168.

[11] J.M.M. Barata, D.F.G. Durão, M.V. Heitor, Impingement of single and twin turbulent jets through a crossflow, AIAA Journal 29 (4) (1991) 595-602.

[12] J.M.M. Barata, Ground Vortex Formation with Twin Impinging Jets, in: International Powered Lift Conference, SAE Paper 962257, November 18-20, 1996, Jupiter, Florida.

[13] J.M.M. Barata, Fountain flows produced by multiple jets in a crossflow, AIAA Journal 34 (12) (1996) 2523-2530.

[14] A.J. Saddington, K. Knowles, P.M. Cabrita, Flow visualization and measurements in a short take-off, vertical landing fountain flow, in: 45th AIAA Aerospace Sciences Meeting and Exhibit, January 8-11, 2007, Reno, Nevada.

[15] H. Tennekes, J.L. Lumley, A First Course in Turbulence, The MIT Press, 1972.

[16] J.M.M. Barata, D.F.G. Durão, Laser-Doppler measurements of a highly curved flow, AIAA Journal 43 (12) (2005) 2652-2655.

[17] J.M.M. Barata, S. Ribeiro, P. Santos, A.R.R. Silva,

Experimental study of a ground vortex, Journal of Aircraft 46 (12) (2009) 1152-1159.

[18] J.M.M. Barata, P.J.C.T. Santos, A.R.R. Silva, The turbulent structure of a ground vortex, in: AIAA 48th Aerospace Sciences Meeting, Paper AIAA-2010-1051, January 4-7, 2010, Orlando, Florida.

[19] A.R.R. Silva, D.F.G. Durão, J.M.M. Barata, P.J.T. Santos, S.D.G. Ribeiro, Laser-Doppler analysis of the separation zone of a ground vortex, International Review of Aerospace Engineering (I.R.E.A.S.E) 2 (3) (2009) 167-174.

[20] B.L. Gilbert, Detailed turbulence measurements in a two-dimensional upwash, in: AIAA 16th Fluid and Plasma Dynamics Conference, AIAA paper 83-1678, July 12-14, 1983, Danvers, Massachusetts.

[21] R.D. Metha, P. Bradshaw, Design rules for small low-speed wind tunnels, The Aeronautical Journal of the Royal Aeronautical Society (1979) 443-449.

[22] W.J. Yanta, R.A. Smith, Measurements of turbulent transport properties with a laser-Doppler velocimeter, in: 11th Aerospace Sciences Meeting, AIAA Paper 73-0169, 1978, Washington.